The Design and Performance of a Wideband Radio Telescope for the GAVRT Program

William A. Imbriale, *Life Fellow, IEEE*, Sander Weinreb, *Life Fellow, IEEE*, Glenn Jones, Hamdi Mani, and Ahmed Akgiray, *Student Member, IEEE*

***Abstract*—A wideband Radio Telescope was designed and built for use in the Goldstone Apple Valley Radio Telescope (GAVRT) program. It uses an existing 34-m antenna retrofitted with a tertiary offset mirror placed at the vertex of the main reflector. It can be rotated to allow using two feeds that cover the 0.5–14-GHz band. The feed for 4.0–14.0 GHz is a cryogenically cooled, commercially available, open-boundary quadridge horn from ETS-Lindgren. Coverage from 0.5 to 4.0 GHz is provided by an uncooled lower frequency version of the same feed that uses a cooled LNA. The measured aperture efficiency is greater than 40% over much of the band.**

***Index Terms*—Noise temperature, quadridge horn, radio telescope, reflector antennas, wideband feeds.**

I. Introduction

THE Goldstone Apple Valley Radio Telescope (GAVRT) outreach project is a partnership involving NASA, the Jet Propulsion Laboratory (JPL), the Lewis Center for Educational Research (LCER), and the Apple Valley Unified School District., located east of Los Angeles, CA, near the NASA Goldstone deep space communication complex. This educational program currently uses a 34-m antenna, DSS12, at Goldstone for classroom radio astronomy observations via the Internet. The GAVRT program [1] introduces students in elementary, middle, and high school to the process of science with the goal of improving science literacy among American students. The current program utilizes DSS12 in two narrow frequency bands around S-band (2.3 GHz) and X-band (8.45 GHz) and is used by a training program involving a large number of secondary school teachers and their classrooms. There is currently a great deal of work going on to develop the next generation Radio Astronomy telescopes, the most notable being the Square Kilometre Array (SKA) [2]: The SKA is considering the use of aperture arrays (AAs), phased array feeds (PAFs), as well as wideband single-pixel feeds. However, since a 34-m antenna was provided to the project at no cost, only wideband feeds for reflector antennas were considered. Also, as the budget was very limited, and only one beam was required, a PAF was not deemed appropriate for this project. The systems coming closest to the planned GAVRT system are probably the ATA [3] or the MeerKat [4] telescopes. However neither of these telescopes is planned for Educational research. To expand the GAVRT program, a joint JPL/LCER project was started in mid-2006 to retrofit an additional existing 34-m beam-waveguide antenna, DSS28, with wideband single-pixel feeds and receivers to cover the 0.5–14-GHz frequency bands.

The DSS28 antenna was designed as part of the JPL Antenna Research System Task described in [5]. The antenna has a 34-m diameter main reflector, a 2.54-m subreflector, and a set of beam waveguide mirrors surrounded by a 2.43-m tube. The antenna was designed for high power and a narrow frequency band around 7.2 GHz. The performance at the low end of the frequency band desired for the educational program would be extremely poor if the beam waveguide system was used as part of the feed system. Consequently, the 34-m antenna was retrofitted with a tertiary offset mirror placed at the vertex of the main reflector. The tertiary mirror can be rotated to allow using two wideband feeds that cover the 0.5–14-GHz band. The feed for 4.0–14.0 GHz is a cryogenically cooled, commercially available, open-boundary Quadridge horn (Model 3164-05) from ETS-Lindgren [6]. The wideband cryogenic LNA [7] has a gain of 35 dB and a noise temperature of 5 K over the majority of the frequency band. The computed aperture efficiency is greater than 40% over most of the band and greater than 55% from 6 to 13.5 GHz. The actual measured efficiency was a bit less ($\sim$40% over most of the band) because of some mirror misalignments and a worse-than-predicted main reflector surface RMS. Coverage from 0.5 to 4.0 GHz is provided by an uncooled, larger version of a similar Lindgren feed (Model 3164-06). This paper will describe the wideband radiometric receiver front-end with emphasis on the feed and optical system.

This paper is a follow on to [8], which describes the RF design of the telescope. The paper adds information on the low frequency feed, describes the installation of the hardware on the telescope, and most importantly, gives the measured efficiency and noise temperature on the telescope itself.

II. Radio Astronomy Applications of the System

Previously, GAVRT only had access to narrow bandwidth S- and X-band radiometers with limited scientific potential. In

Manuscript received January 03, 2010; revised January 30, 2011; accepted January 31, 2011. Date of publication March 14, 2011; date of current version June 02, 2011. This work was carried out at the Jet Propulsion Laboratory, California Institute of Technology, Pasadena, under a contract with the National Aeronautics and Space Administration.

W. A. Imbriale is with the Jet Propulsion Laboratory, California Institute of Technology, Pasadena, CA 91109 USA (e-mail: imbriale@jpl.nasa.gov).

S. Weinreb, G. Jones, and A. Akgira are with the California Institute of Technology, Pasadena, CA 91125 USA (e-mail: sweinreb@caltech.edu; jones_gl@caltech.edu; ahmed@caltech.edu).

H. Mani is with Arizona State University, Tempe, AZ 85287 USA (e-mail: mani@gmail.com).

Color versions of one or more of the figures in this paper are available online at http://ieeexplore.ieee.org.

Digital Object Identifier 10.1109/TAP.2011.2123863

contrast, DSS-28 has been outfitted with a novel wide bandwidth receiver which enables a wide range of scientific campaigns, encouraging broader participation from the scientific community. The scientific observations that are enabled by the 0.5–14-GHz frequency range are the following.

1) *Quasar variability study:* Long-term flux monitoring at multiple frequencies can help to understand intrinsic variability versus effects of the interstellar medium.
2) *Jupiter quest:* Long-term flux measurements to study synchrotron emission from Jupiter.
3) *Giant pulses from the crab pulsar:* Wide bandwidth provides new insight into this phenomenon. Long-term statistical study will be combined with gamma-ray data from the Fermi telescope to look for correlation.
4) *Spectral lines:* Many spectral lines can be simultaneously observed. This could be used to search for radio sources and to monitor molecular masers which may vary on week to month timescales.

III. System Design

The complete system involves the reflector, subreflector, tertiary reflector, feed, cryogenics subsystem, low noise amplifiers, noise calibration system, frequency converters, digital spectrometers, continuum signal processing, and monitor and control system. Only the optics design, tertiary mirror, feeds, cryogenics, and LNA will be discussed in this paper. Further information on the rest of the system can be found in [9]. The main parameters of this front-end are the antenna efficiency η and the system noise temperature Tsys. The goal was an η of $> 40\%$ from 1 to 14 GHz and a maximum Tsys of 55 K over the band with 35 K as a goal.

In order to meet the above Tsys requirement, the wideband feed (which has more ohmic and mismatch loss than a typical narrow band feed such as a corrugated horn) needs to be cryogenically cooled, at least for frequencies above 4 GHz. The baseline approach will utilize two feeds, a commercially available feed to cover the 4–14-GHz range which is cryogenically cooled and a second feed (a scaled version of the higher frequency feed) which is not cryogenically cooled. However, even though the lower frequency feed is not cooled, the LNA amplifier is cooled.

The wideband LNA's required for the system have been under development for many years and over 100 units of the type used in this system have been assembled, tested at 15 K, and utilized in radio astronomy and physics research systems [4]. When cooled to 15 K, the noise is under 5 K from 1 to 12 GHz when driven from a 50-Ω generator.

IV. Optics Design Tradeoffs

The antenna to be retrofitted is a 34-m beam waveguide antenna designed as part of the JPL Antenna Research System Task described in [5]. The original antenna geometry used a beam waveguide feed system that consisted of a paraboloid and three flat mirrors. The radiation from the feed horn is allowed to spread to the paraboloid, where it is focused to a point at infinity. Hence, after reflection, a collimated beam exists that is directed to the subreflector by the three flat reflectors. The energy is contained in the 2.743-m diameter of the BWG tube and does not begin to spread significantly until it exits through the main reflector. Since a collimated beam exists beyond the first mirror, this antenna is closely related to a near-field Cassegrain design, where the feed system is defined to include both the feed horn and a parabolic mirror.

Because of the near-field Cassegrain design, both the main reflector and the subreflector are nominally paraboloids, with dual-reflector shaping used to increase the illumination efficiency on the main reflector by compensating for the amplitude taper of the feed radiation pattern. The design of the dual-shaped antenna is based upon geometrical optics, with the shape of the subreflector chosen to provide for uniform amplitude illumination of the main reflector, given the distribution of the radiation striking the subreflector. The curvature of the main reflector is then modified slightly from that of the parent paraboloid to compensate for any phase errors introduced by the subreflector shaping.

The antenna was designed for high power and a narrow frequency band around 7.2 GHz. The performance at the low end of the frequency band desired for the educational program would be extremely poor if the beam waveguide system was used as part of the feed system. Hence, several redesign options to enable improved performance on the low frequency without the use of the beam waveguide itself were examined as described in [8]. They included: 1) redesigning the subreflector and using the broadband feed in a dual reflector system; 2) using a symmetric 2.54-m reflector tertiary reflector placed at the dish vertex; 3) using a 90° 2.54-m offset design tertiary reflector at the dish vertex; 4) replacing the upper flat mirror with a parabola and placing the feed in the upper portion of the beam waveguide tube; and 5) using a 60° 2.3-m tertiary mirror at the dish vertex. Relative performance was computed using an idealized feed pattern that approximated the type of feed to be used.

Purely from an efficiency standpoint, the feed placed at the focal point of a shaped dual reflector antenna was best. However, since the optics design of the existing system did not have a usable focal point, the subreflector would have to be replaced with one with an appropriate design and the main reflector panels reset for the new subreflector design. Also, since the feed has a very broad pattern, the feed would need to be placed near the subreflector necessitating the use of a tall feed tower to support it, or hanging the feed from the subreflector. Also, it would be difficult to access the feed system for maintenance and replacement. For both cost and logistical reasons, this option was rejected.

The next best performing option was a symmetric parabola placed at the vertex of the dish. Since the feed blockage would be small, the only other disadvantage of this option was that it would not be able to easily switch between feeds if, to cover the frequency band, more than one feed would be required. The offset options allowed the use of a rotating reflector that would be able to easily switch between multiple feeds. Since this is to be an educational tool, flexibility and versatility are extremely important. Hence, this option was rejected.

For the offset options, the parabola at the flat mirror position performed poorly at the lowest frequencies. The performance

Fig. 1. Two feeds and tertiary mirror at the vertex of the main reflector.

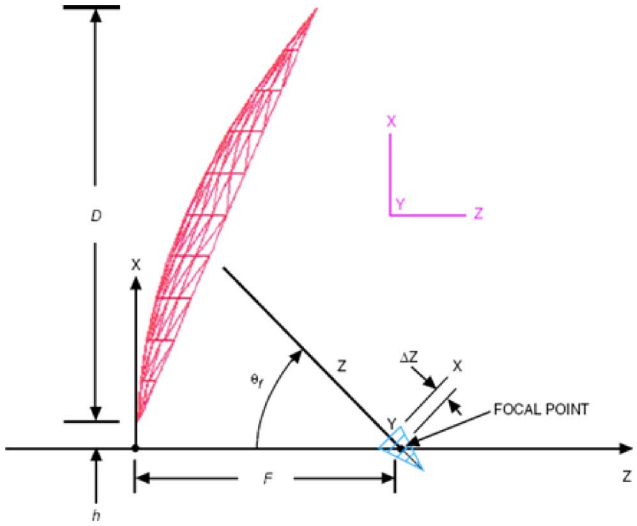

Fig. 2. Geometry of the tertiary mirror.

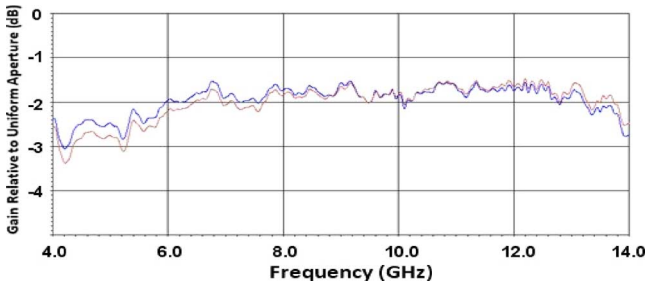

Fig. 3. Comparison of the tertiary reflector optimized for 4 GHz (dark curve) and 12 GHz (light curve).

for the other two offset options was virtually identical, so the design with the smaller parabola was selected.

Thus, the design chosen was to use an offset tertiary mirror placed at the vertex of the main reflector as shown in Fig. 1. The tertiary is fed by a commercially available wideband feed from Lindgren. There are two feeds used, one for the lower band and one for the higher band. The tertiary mirror is rotated to switch between the feeds.

Prior to the selection of the Lindgren feed, several other feed options were considered. The original idea was to use the Eleven feed as described in [10]. However, when the Eleven feed was married to the LNA and placed in a cryogenic Dewar, the noise temperature of the feed system was unacceptably high. This was at an early stage in the development of the feed, and the high noise temperature was probably due to the very thin feed lines which did not provide adequate heat transfer from the feed to the cold stage of the cryogenic system. Since then, further work has been done [11], but much too late for this project. The ATA log-periodic dipole feed [12] was also considered. However, the ATA feed had a very complex and delicate integration of the LNA with the feed. The Lindgren feed, being all metal and quite robust, allowed a simple integration of the feed and LNA, and the entire feed was able to be cooled to cryogenic temperatures.

V. Optics Design Optimization

Amplitude and phase, copolar and cross-polar patterns of the Lindgren feed were measured at phi angles of 0°, 45°, 90°, and 135° and for theta rotation angles of $-180°$ to $+180°$ in 10° steps. The data was taken for the feed with absorber strips on the fin outer surfaces and a metal cylinder surrounding the feed. This data was then used to optimize the design of the tertiary reflector whose parameters are shown in Fig. 2. Of the two feed systems, the higher priority was the high frequency feed; hence the tertiary was optimized for the high frequency performance accepting whatever performance resulted at the lower frequency bands. Near the ends of the high frequency band, 4 and 12 GHz, were selected for the optimization. The parameters to be optimized were focal length, diameter, offset height, feed tilt angle, and feed defocusing. An optimization program was used and the parameters determined that yielded the highest peak gain. Using the geometry shown in Fig. 2, the optimum parameters for 4 GHz are $\mathrm{F} = 1.38$ m, $\mathrm{D} = 2.24$ m, $\theta_\mathrm{f} = 47°$, $\mathrm{h} = 7.7$ cm, and $\Delta\mathrm{z} = -.32$ cm. The optimum parameters for 12 GHz are $\mathrm{F} = 1.27$ m, $\mathrm{D} = 2.25$ m, $\theta_\mathrm{f} = 49.3°$, $\mathrm{h} = 8.7$ cm, and $\Delta\mathrm{z} = 1.12$ cm. Data for the Lindgren feed was taken every 50 MHz from 2 to 22 GHz and the calculated performance for the two designs shown in Fig. 3. It should be noted that the data shown in Fig. 3 only includes the physical optics parameters that vary with the tertiary parameters. A more complete estimate of performance will be given later. Since the parameters of the two designs were so close, the optimized design at 12 GHz was used as the final design. The performance at 4 GHz using this design was virtually identical to its optimum design.

VI. High-Frequency Feed (HFF) and Test Results

Pattern and noise measurements of the ETS-Lindgren Model 3164-05 antenna designed by Rodriguez [6] will be described in this section. Integration of the feed with the cryogenics dewar can have a large effect upon the performance. The mechanical configuration is shown in Figs. 4 and 5. Other than Teflon in the SMA connector, the feed is constructed entirely of aluminum and no deleterious effects of the cryogenic cooling are expected. Within the outer dewar aluminum cylinder vacuum jacket, there is an aluminum radiation shield of diameter 24.1 cm to prevent thermal coupling of the feed to 300 K. Thermal radiation, of the order of 20 W, enters the window, but is mostly blocked by a blanket consisting of 16 layers of 25-μm-thick Teflon film

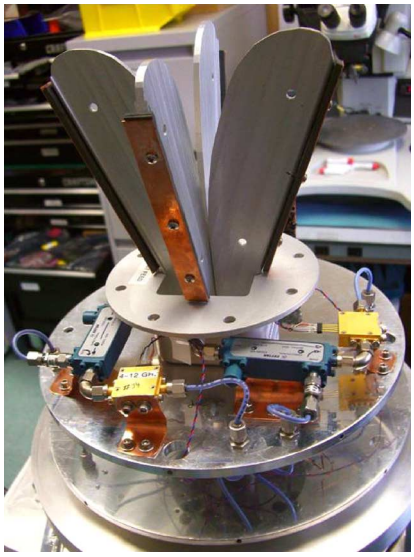

Fig. 4. Cryogenic wideband feed and LNA.

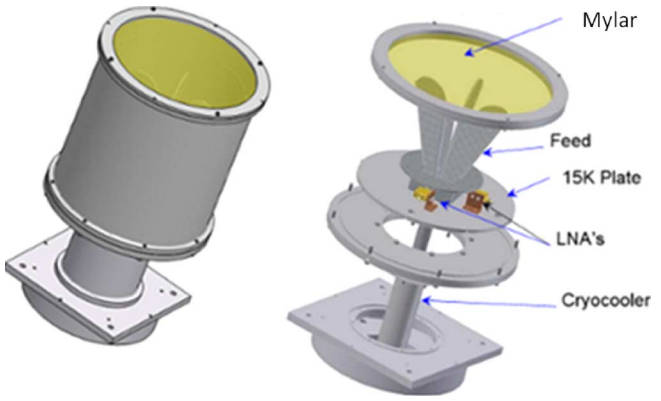

Fig. 5. Integration of feed in a cryogenic dewar with 30-cm outside diameter.

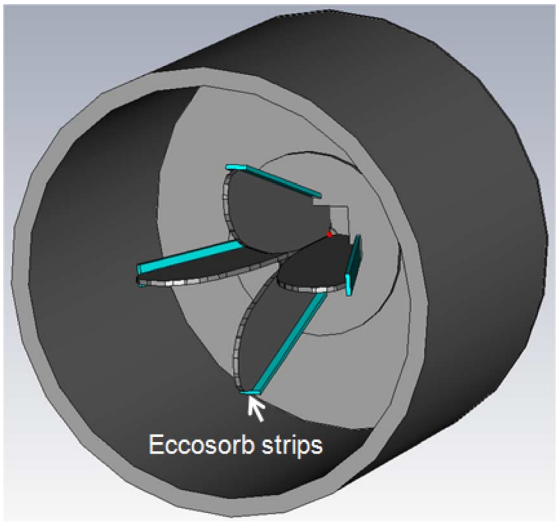

Fig. 6. Configuration of feed simulated by CST.

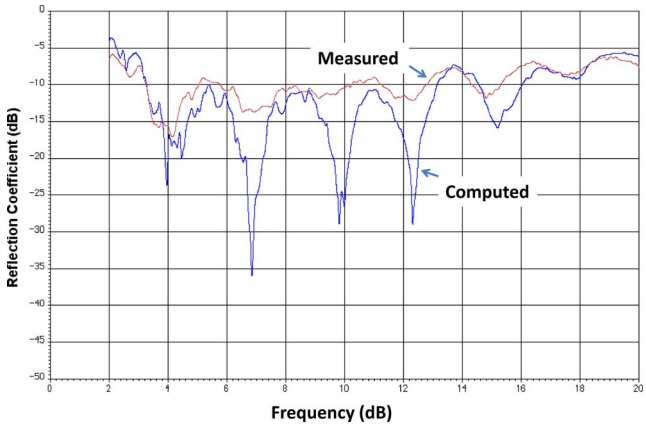

Fig. 7. Feed reflection coefficient.

separated by a mesh of fine French wedding veil. Without this blanket, it was not possible to cool the feed below 100 K, but with the blanket, the temperature measured on the feed was 21 K. The total thickness of Teflon is thus 0.4 mm, and with dielectric constant of 2.1, the total electrical length is $\lambda/38$ at 14 GHz, which will produce negligible reflections. The window material is 0.35-mm MYLAR. The window electrical length of $\lambda/34$ at 14 GHz is negligible. The total force on the window at 15 psi atmospheric pressure is 1140 lbs, which produces a perimeter radial stress of 3097 psi compared to a 28 000-psi yield stress for MYLAR.

The feed, the surrounding cylinder and the Eccosorb was simulated using the CST Studio time-domain electromagnetic simulation software. The configuration is shown in Fig. 6. The dewar vacuum jacket inner diameter is 28 cm, the radiation shield diameter is 24.1 cm, the dewar length from the bottom of the feed base to the top of the dewar is 19.7 cm, and the feed length from bottom of base to top of fin is 17.3 cm .The Eccosorb FDS strips are $125 \times 15 \times 3$ mm^2. The feed reflection coefficient without window was measured and compared to the calculation as shown in Fig. 7. JPL has extensively used MYLAR windows, and they have been shown to have negligible effect on the return loss. The 2.4-GHz ripple period in the data would arise from two reflections spaced 6.2 cm apart, which is of the order of the spacing of the connector to the radiating region of the slot. The feed has a built-in balun and could be better matched with a differential LNA. Effects of the feed impedance variation are observed in the noise data and improvements in the noise match to the LNA for particularly important frequencies could be implemented.

The feed patterns were measured with several different configurations of surrounding structures. The feed patterns were tested with a surrounding cylinder, the cylinder lined with absorber, and in the cylinder but with absorbing strips taped to the outer rim. All pattern measurements were made in a small chamber at Caltech. Efficiency calculations of the complete antenna system were performed using pattern measurements with the feed and absorber strips in a cylinder. It was found that the pattern for illumination of a reflector could be improved by surrounding the feed with an absorbing cylinder. At a later stage, it was realized that placing absorbing strips of lossy material on the outer surfaces of the fins could have the same effect. Currents flowing around the outer perimeter of the fins are thus absorbed and prevented from coupling to the surrounding cylinder. The question is raised as to whether the absorber will deteriorate the

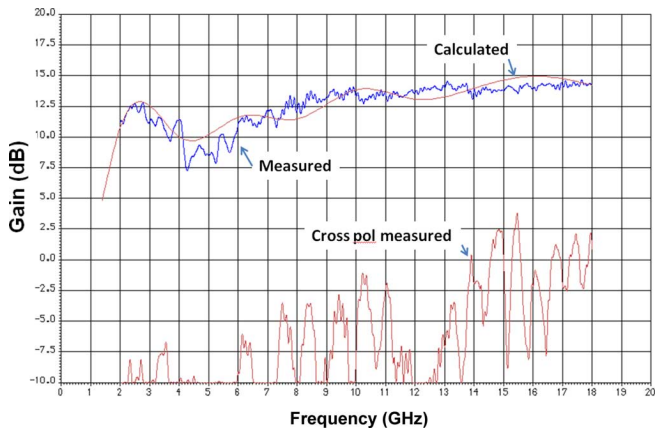

Fig. 8. Comparison of computed and measured feed gain.

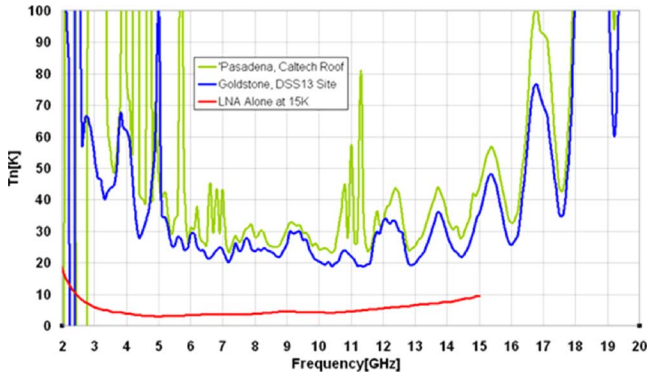

Fig. 9. Noise temperature of feed and LNA as a function of frequency for measurements in Pasadena (top), Goldstone, and of the LNA alone measured at 15 K referred to its coaxial input jack.

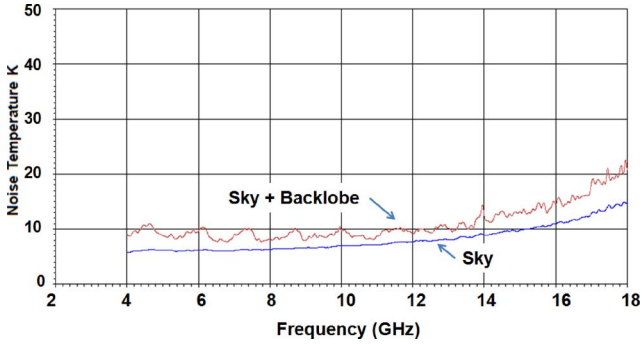

Fig. 10. Noise contribution from the sky and backlobe of the feed.

efficiency of the feed and add to the noise temperature. Data indicating that the efficiency may not be reduced was obtained by measuring the transmission loss from the feed to a test antenna in an anechoic chamber. Compared to the case with no absorber, the result shows a decrease in transmission loss at frequencies below 3 GHz, small increase in loss from 3 to 6 GHz, and negligible effects above 6 GHz. The noise temperature contributed by the absorber should be small if the absorber is at cryogenic temperatures. A comparison of the computed and measured feed gain is shown in Fig. 8. Performance of the complete reflector system performance will be shown in a later section.

After the pattern tests, the feed was integrated with LNA's on both polarizations and a cryogenics dewar cooled with a closed-cycle CTI Model 350 cryocooler. This cooler has a capacity of 2 W at 14 K and 5.5 W at the measured temperature of 21 K. Cool-down time was approximately 6 h.

Noise temperature tests of the cooled system were performed both in Pasadena, CA, and later in the Mohave Desert at Goldstone, CA, to reduce the effects of radio frequency interference (RFI). One polarization had a 4–12-GHz LNA, with 39 dB gain and <10 K noise from 3 to 14 GHz increasing to 20 K noise at 2 GHz, while the other polarization had a modified 0.5–11-GHz LNA (labeled the 2–12-GHz LNA) , also with 39 dB gain and <10 K noise from 3 to 14 GHz, but with 15 K noise at 2 GHz. It is possible that the intense RFI may have affected some of the noise measurements.

The measured noise temperature results are shown in Fig. 9 for data taken in Pasadena, at Goldstone, and for the LNA alone. The peaks in the Pasadena curve at the low frequencies and around 11 GHz are primarily due to RFI, whereas the residual ripple in the Goldstone curve is due to matching. The slightly worse contribution from Pasadena (Caltech roof) is probably due to there being more obstructions near the feed contributing to more noise temperature from the backlobe scatter. The data taken at Pasadena and Goldstone utilized the standard Y-factor technique for measuring Tsys and then subtracting an assumed sky contribution of 5 K. However, as seen in Fig. 10, which shows calculated contribution (using measured feed data) from the sky, the actual sky contribution is greater than 5 K. Fig. 10 also shows the calculated contribution from the feed backlobe. Notice that the Goldstone curve of Fig. 9 is mostly around 20 K, and the LNA about 5 K. The ~15-K difference is made up of: 1) the feed backlobe of ~3–5 K; 2) the ~2–4 K of greater than assumed 5-K noise for the sky; and 3) a combination of feed loss (including edge absorber strips), losses in the couplers, Teflon blanket, and window. The feed plus LNA noise is <35 K from 4.2 to 15 GHz and is less than 25 K in most of the band. These results are consistent with the Tsys goals (on 34-m telescope including sky and spillover) of <55 K up to 14 GHz and 35 K at best frequencies.

VII. Low Frequency Feed (LFF)

This section describes the performance of the low frequency feed (LFF). The LFF covers the 0.5–4-GHz band and is intended to be a low-frequency version of the HFF. Consequently, the ETS Lindgren 3164-06 (0.3–6 GHz) was selected. The feed is not cooled, but the LNA is cooled. As with the HFF, the feed is surrounded by an aluminum cylinder to improve the pattern. The reflection coefficient and E- and H-plane patterns were simulated using the CST Studio time-domain electromagnetic simulation software. The LFF is shown in Fig. 11. The cylinder inner diameter is 71 cm; cylinder length from bottom of feed base to top of the cylinder is 51 cm. The cylinder top and feed top are flush. The computed and measured return loss is shown in Fig. 12. This feed has both a poor return loss and poor radiation patterns around 3 GHz. This has a significant impact on the telescope performance as will be shown in the following section. The HFF has no similar problem. A long-term plan is to replace this feed with a feed that performs more like the HFF.

Fig. 11. Low frequency feed.

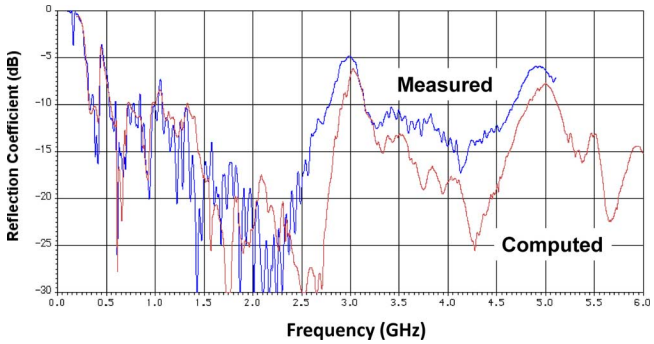

Fig. 12. LFF reflection coefficient.

The receiver system was taken to the DSS13 area of the NASA Goldstone site, Ft. Irwin, CA, on November 29, 2007, for tests of the receiver noise temperature by the Y-factor method comparing the receiver output on a spectrum analyzer (Agilent E4407) covering the feed with ambient temperature absorber and then removing the absorber to view cold sky. The feed is uncooled, but the LNA's for both polarizations are cooled in the small rectangular dewar placed under the cylinder. The noise temperature of the feed plus LNA is shown in Fig. 13. The measured system temperature implies a total loss of 0.4 dB at 300 K in cables to the feed and in the feed.

VIII. LNAs

Fig. 14 shows the cryogenic low noise amplifier used in the HFF system [9]. The amplifier was designed at Caltech, and the 0.1-μm InP HEMT MMIC is fabricated by Northrop Grumman. The noise is under 7 K and gains over 35 dB from 1–12 GHz when cooled to 15 K. The input 1-dB gain compression point is above -40 dBm, and the power consumption is 22 mW. Over 100 of these LNA's have been constructed and are in use at other radio observatories.

Fig. 15 shows the noise temperature versus frequency for the SiGe low noise amplifier used in the GAVRT low frequency (LFF) receiver [13]. Two such LNAs, one for each polarization, are cooled to approximately 60 K by a compact Stirling cycle cooler manufactured by Sunpower; the feed and cables

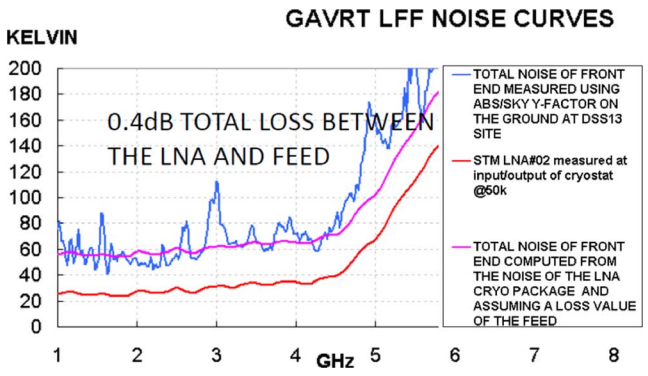

Fig. 13. Feed plus LNA noise temperature. The 30 K of additional noise when the feed is included is due to loss of coaxial lines from LNA to feed (estimate 0.2 dB), feed loss (estimate 0.1 dB), and a small amount of 300-K ground radiation due to scattering from the rim of the cylinder shield.

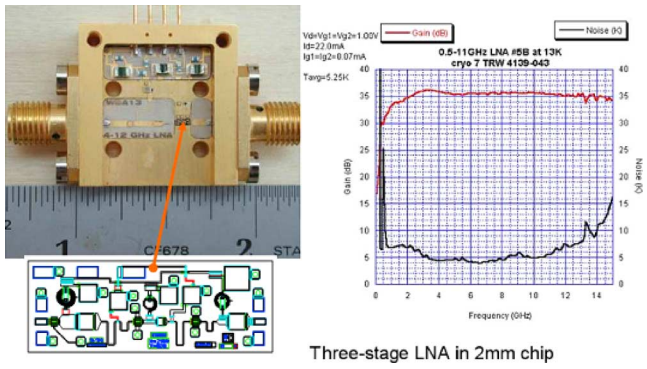

Fig. 14. Cryogenic low noise amplifier used in the HFF system.

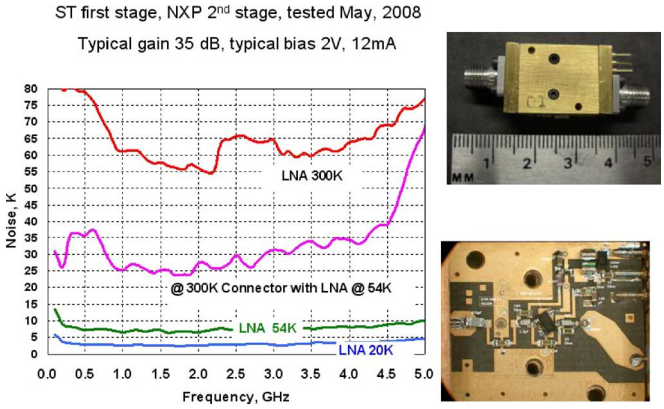

Fig. 15. Low frequency LNA.

the feed are uncooled. The LNA noise temperature measured at the cold input jack is ~8 K, but this is increased to ~30 K by internal thermal transitions and a vacuum coaxial feedthrough. The external cables, losses in the feed, and antenna temperature increase the total system noise to the 60–100 K range as shown in Fig. 13.

IX. Efficiency and Noise Temperature Measurements

The methodology for the efficiency and noise temperature measurements is described in [6]. The results will be summarized here along with a comparison to the computed results.

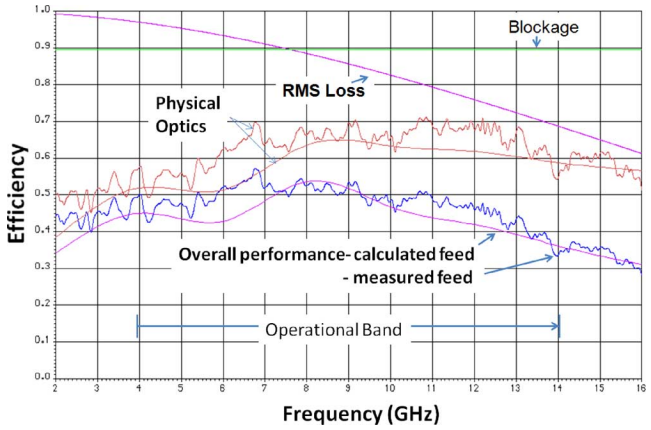

Fig. 16. Computed performance of the HFF showing loss components.

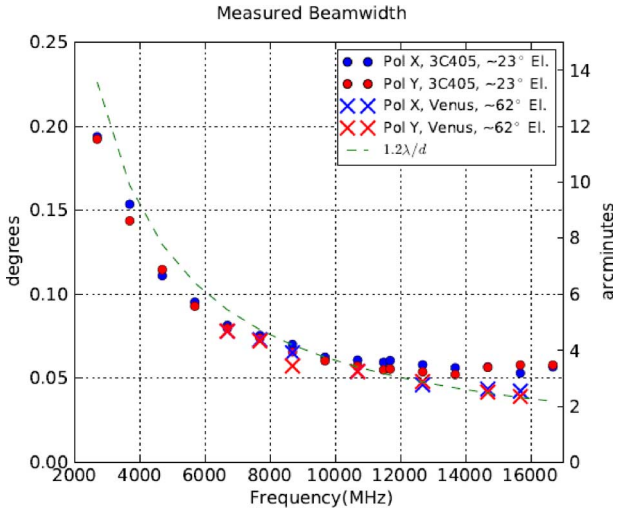

Fig. 17. Beamwidth of the DSS-28 high frequency feed measured on Venus and the radio galaxy Cygnus A (3C405).

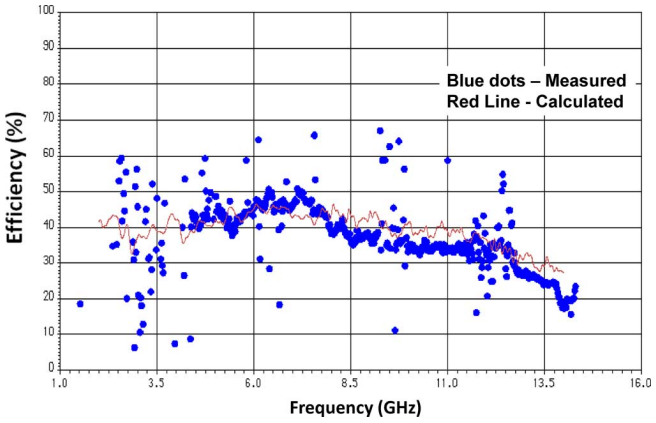

Fig. 18. Comparison of computed and measured efficiency for the HFF.

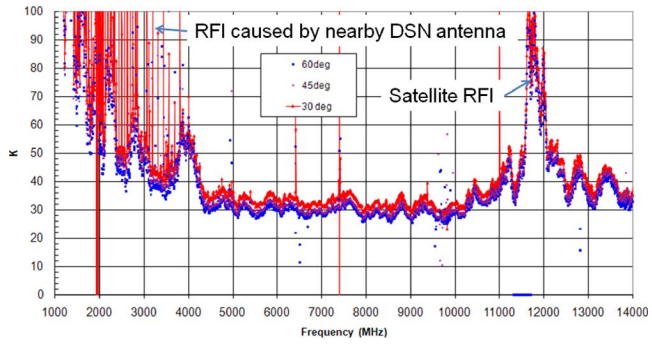

Fig. 19. Measured noise temperature of the HFF on DSS-28.

The calculated data shown in Fig. 3 only included the physical optics parameters that would vary with the tertiary parameters. It did not include some of the other losses present in the complete antenna system such as blockage and RMS error. A more complete efficiency estimate is shown in Fig. 16 for the high frequency feed. It includes a calculation using the measured feed patterns along with a comparison using the calculated feed patterns.

The measured efficiency of the High Frequency Feed was determined by measuring the response of the system to the radio galaxy 3C405 and Venus. The 3C405 measurements were made at an elevation of approximately 23°, while those on Venus were made at approximately 62°. After correcting any pointing offsets by manually peaking the response of the telescope on the source, the telescope was moved off source by one degree in cross elevation. The high-power noise calibration signal was pulsed to measure the system gain, and then the telescope was commanded to scan through the source in cross elevation at a fixed rate. Finally, at the end of the scan, the noise source was pulsed again. To process the data, the system gain was estimated from the calibration signal responses using a lookup table to determine the calibration signal value in Kelvin. A Gaussian was then fit to the scan data including a constant offset for the system temperature and a linear baseline to account for drift during the scan. The peak of the Gaussian provided the antenna temperature of the source, and the width of the Gaussian was used to compute the beamwidth. The measured beamwidth on Venus and the radio galaxy Cygnus A (3C405) is shown in Fig. 17. The beamwidth computed from $1.2\lambda/\mathrm{d}$ (a standard rule of thumb) is plotted for comparison. Notice that the beamwidth becomes comparable to the angular extent of Cygnus A at around 10 GHz.

Fig. 18 compares the measured efficiency of the high frequency feed to the calculated performance using the measured feed patterns. The efficiency data is an ensemble of several sources and several elevation angles. The wide spread in the measured data is primarily due to RFI. There was some misalignment in the tertiary mirror (measured using photogrammetry) and the effect of the misalignment is included in the calculated data and accounts for the difference between the data shown in Fig. 16. The misalignment accounts for about a 5% loss at the higher frequencies and will be recovered when the system is realigned. The measured data is in excellent agreement with the calculated data.

Fig. 19 shows the measured noise temperature of the HFF on DSS-28. Comparing Fig. 19 to Fig. 9, it can be seen that the antenna noise temperature contribution is less than 10 K, which is typical for the 34-m antennas in the Deep Space Network.

Fig. 20 shows the aperture efficiency, and Fig. 21 the system temperature of the Low Frequency Feed measured on Cygnus

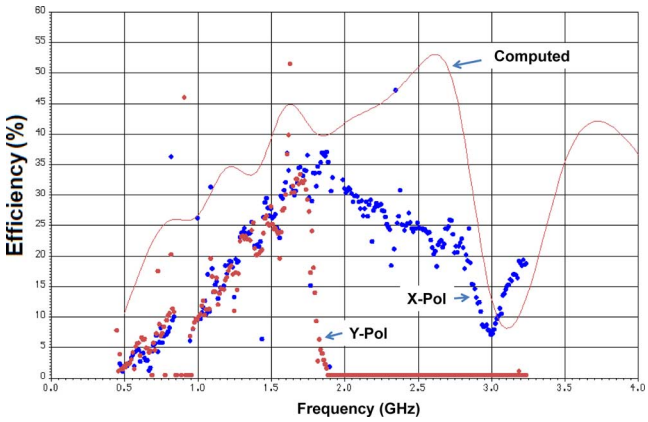

Fig. 20. Computed and measured performance of the low frequency system at DSS-28.

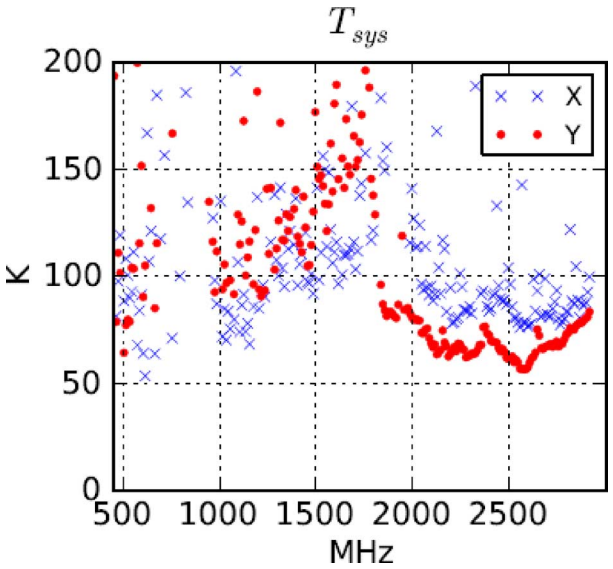

Fig. 21. System noise temperature of the LFF.

A (3C405). The sharp cutoff in the efficiency measured on polarization Y is due to a low pass filter installed between the feed and LNA to combat RFI. The calibration signal was injected after the filter so the system temperature could be measured above the filter cutoff frequency. The linear drop in efficiency below 1 GHz is a result of the secondary reflector being too few wavelengths across and is clearly displayed in the calculated data. The large scatter in the points is largely due to RFI, which is especially problematic in this frequency range due to a nearby 34-m DSN antenna that transmits S-band. The effect of the poor feed performance at 3 GHz can also be clearly seen in the measured data. It is clear from the calculated and measured data that the low frequency feed did perform as advertised and consequently did not act like a scaled version of the HFF.

X. Conclusion

A 34-m antenna was retrofitted with a tertiary offset mirror placed at the vertex of the main reflector. The tertiary mirror can be rotated to allow using the two feeds that cover the 0.5–14-GHz band. The feed for 4.0–14.0 GHz is a cryogenically cooled, commercially available, open-boundary Quadridge horn from ETS-Lindgren. The wideband cryogenic LNA has a gain of 35 dB and a noise temperature of 5 K over the majority of the frequency band. Coverage from 0.5 to 4.0 GHz is provided by an uncooled, lower frequency Lindgren feed. The computed aperture efficiency of the high frequency feed is greater than 40% over most of the band and greater than 55% from 6 to 13.5 GHz. The actual measured efficiency was a bit less (∼40% over most of the band) because of some mirror misalignments and a worse-than-predicted main reflector surface RMS. The measured zenith noise temperature is below 35 K from 4.3 to 10.5 GHz.

The low frequency feed suffers significantly from RFI and the fact that the tertiary mirror is too small for frequencies below 1 GHz. Also, the low-frequency Lindgren feed did not perform as advertised. The low frequency feed will probably be replaced with a version that performs closer to its higher frequency model It should be noted, however, that the LFF should still be quite effective for observing giant pulses from the Crab pulsar because the flux from the surrounding nebula is so great that it will still dominate the system temperature despite the low efficiency.

Acknowledgment

The authors would like to acknowledge M. Britcliffe for the original idea to put a parabola and feed at the vertex of the 34-m antenna.

References

[1] "Lewis Center for Educational Research," Apple Valley, CA [Online]. Available: http://www.lewiscenter.org/gavrt/

[2] "The Square Kilometre Array," SKA, Manchester, U.K. [Online]. Available: http://www.skatelescope.org/

[3] W. J. Welch, D. Backer, L. Blitz, D. C.-J. Bock, G. C. Bower, C. Cheng, S. Croft, M. Dexter, G. Engargiola, E. Fields, J. Forster, C. Gutierrez-Kraybill, C. Heiles, T. Helfer, S. Jorgensen, G. Keating, J. Lugten, D. MacMahon, O. Milgrome, D. Thornton, L. Urry, J. van Leeuwen, D. Werthimer, P. H. Williams, M. Wright, J. Tarter, R. Ackerman, S. Atkinson, P. Backus, W. Barott, T. Bradford, M. Davis, D. DeBoer, J. Dreher, G. Harp, J. Jordan, T. Kilsdonk, T. Pierson, K. Randall, J. Ross, S. Shostak, M. Fleming, C. Cork, A. Vitouchkine, N. Wadefalk, and S. Weinreb, "The Allen telescope array: The first widefield, panchromatic, snapshot radio camera for radio astronomy and SETI," *Proc. IEEE*, vol. 97, no. 8, pp. 1438–1447, Aug. 2009.

[4] J. L. Jonas, "MeerKAT—The South African array with composite dishes and wide-band single pixel feeds," *Proc. IEEE*, vol. 97, no. 8, pp. 1522–153, Aug. 2009.

[5] W. A. Imbriale, *Large Antennas of the Deep Space Network*. Hoboken, NJ: Wiley, 2003, ch. 9.

[6] V. Rodriguez, "A multi-octave open-boundary quad-ridge horn antenna for use in the S to Ku-bands," *Microw. J.*, vol. 49, no. 3, pp. 84–92, Mar. 2006.

[7] J. D. Pandian, L. Baker, G. Cortes, P. F. Goldsmith, A. A. Deshpande, R. Ganesan, J. Hagen, L. Locke, N. Wadefalk, and S. Weinreb, "Low-noise 6–8 GHz receiver," *IEEE Microw. Mag.*, vol. 7, no. 6, pp. 74–84, Dec. 2006.

[8] W. A. Imbriale, S. Weinreb, and H. Mani, "Design of a wideband radio telescope," in *Proc. IEEE Aerosp. Conf.*, Mar. 3–10, 2007, pp. 1–2.

[9] G. Jones, "Instrumentation for wide bandwidth radio astronomy," Ph.D. dissertation, Dept. Elect. Eng., California Institute of Technology, Pasadena, CA, 2010.

[10] R. Olson, P. S. Kildal, and S. Weinreb, "The Eleven antenna: A compact low-profile decade bandwidth dual polarized feed for reflector antennas," *IEEE Trans. Antennas Propag.*, vol. 54, no. 2, pp. 368–375, Feb. 2008.

[11] C. Beaudoin, P.-S. Kildal, J. Yang, M. Pantaleev, and B. Klein, "Ongoing work with the cryogenic eleven antenna at the MIT Haystack Observatory," in *Proc. Int. Workshop Phased Array Antenna Syst. Radio Astron.*, Provo, UT, May 3–5, 2010.

[12] G. Engargiola, "Non-planar log-periodic antenna feed for integration with a cryogenic microwave amplifier," in *Proc. IEEE Antennas Propag. Soc. Int. Symp.*, 2002, vol. 4, p. 143.

[13] S. Weinreb, J. C. Bardin, H. Mani, and G. Jones, "Matched wideband low noise amplifiers for radio astronomy," *Rev. Sci. Instrum.*, vol. 80, p. 044702, Apr. 2009.

William A. Imbriale (S'64–M'70–SM'91–F'93–LF'08) received the B.S. degree in engineering physics from Rutgers University, New Brunswick, NJ, in 1964, the M.S. degree in electrical engineering from the University of California, Los Angeles, in 1966, and the Ph.D. degree from the University of Illinois at Urbana–Champaign in 1969.

He is a Senior Research Scientist with the Communications Ground System Section, Jet Propulsion Laboratory (JPL), Pasadena, CA. Since starting at JPL in 1980, he has led many advanced technology developments for large ground-station antennas, lightweight spacecraft antennas, and millimeter-wave spacecraft instruments. He has recently returned from a six-month sabbatical with Cornell University, Ithaca, NY, where he supported the design of the Square Kilometre Array and is continuing that work at JPL. Prior to the sabbatical, he was a Principle Investigator (PI) on a technology contract for the Earth Sciences Technology Office (ESTO) to develop a subreflector consisting of MEMS switches integrated with patch reflectarray elements that will compensate, in real time, for on-orbit distortions of a membrane inflatable antenna. He was also the Lead Engineer for the Spanish-supplied High Gain Antenna System for the Mars Science Laboratory (MSL) rover. Earlier positions at JPL have included being the Assistant Manager for Microwaves in the Ground Antennas and Facilities Engineering Section and the Manager of the Radio Frequency and Microwave Subsystem Section. Prior to joining JPL, he was with the TRW Defense and Space Systems Group, where he was the Subproject Manager for the Antennas of the TDRSS program. He has lectured and taught engineering courses at several learning institutions, including the University of California, Los Angeles, and the University of Southern California, Los Angeles. He is also a consultant to industry on all aspects of antenna analysis and design.

Dr. Imbriale has received numerous NASA honor awards, including the Exceptional Service Medal. From 1993 through 1995, he was a distinguished lecturer for the Antennas and Propagation Society, speaking on beam-waveguide antennas and the evolution of the Deep Space Network antennas. He was a member of the Administration Committee of the IEEE Antennas and Propagation Society and General Chairman of the 1995 International IEEE Antennas and Propagation International Symposium, held in Newport Beach, CA. He has published extensively and has won three best paper awards.

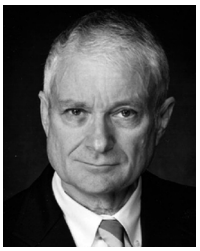

Sander Weinreb (S'56–M'63–SM'71–F'78–LF'02) received the B.S.E.E. and Ph.D. degrees in electrical engineering from the Massachusetts Institute of Technology, Cambridge, in 1958 and 1963, respectively.

He is presently a Principal Scientist with the Jet Propulsion Laboratory (JPL) and a Faculty Associate with the California Institute of Technology (Caltech), Pasadena. Prior to this, he was a Research Professor with the Department of Physics and Astronomy, University of Massachusetts, Amherst. Prior to joining the University of Massachusetts, during 1989–1996, he was Principal Scientist and Leader of the Millimeter-Wave Design and Test Group with Martin Marietta Laboratories, Baltimore, MD, where he led the design of millimeter-wave MMICs and prototype radar and radiometer systems. During 1988 and 1989, he was a Visiting Professor with the University of Virginia, Charlottesville. Prior to this, he was Head of the Electronics Division (1965–1985) and Assistant Director (1985–1988) with the National Radio Astronomy Observatory (NRAO), Charlottesville, VA, where he was responsible for the design, construction, operation, and maintenance of radio astronomy receivers at the Green Bank, WV, and Kitt Peak, AZ, observatories. At NRAO, he led the group responsible for the design of the electronics system for the Very Large Array. He is the author of over 120 publications in the areas of digital correlation techniques, radio astronomy observations, array receivers, and low-noise amplifiers. His main present area of research is the development of low-noise microwave and millimeter-wave integrated circuits (MMICs) for use in radio astronomy and atmospheric research.

Glenn Jones received the B.S. degree in mathematics and engineering and Ph.D. degree in electrical engineering from the California Institute of Technology (Caltech), Pasadena, in 2003 and 2010, respectively.

He is currently a Jansky Post-Doctoral Fellow with the National Radio Astronomy Observatory and is resident at Caltech. He is leading a campaign to study pulsars with the Goldstone Apple Valley Radio Telescope. Previously, he with the Jet Propulsion Laboratory, Pasadena, CA, from 2003 to 2005, working on antenna arrays for deep space communication. His primary area of interest is radio astronomy instrumentation, particularly digital signal processing.

Dr. Jones is a member of the International Union of Radio Science (URSI).

Hamdi Mani is currently pursuing the Ph.D. degree in physics at Arizona State University (ASU), Tempe.

He is with the Terahertz Aastronomy Instrumentation and the Cosmology Laboratories, ASU. He was a Research Technician with the Department of Electrical Engineering, California Institute of Technology (Caltech), Pasadena, from 2005 to 2010. While at Caltech, his activity involved the construction and testing of MMIC cryogenically cooled very low noise amplifiers, microwave noise measurements and calibrations, and the integration of radio astronomy receivers.

Ahmed Akgiray (S'11) received the B.S. degree in electrical engineering from Cornell University, Ithaca, NY, in 2005, the M.S. degree in electrical engineering from the University of Illinois at Urbana–Champaign in 2007 with a thesis titled "Calibration of Jicamarca Radar Using *F*-region Incoherent Scatter For Measurements of *D*-region Backscatter RCS," and is currently pursuing the Ph.D. degree focusing on wideband antenna and LNA development at the California Institute of Technology, Pasadena.

He was with the Jet Propulsion Laboratory, Pasadena, CA from May 2007 to May 2010. His responsibilities included Lead RF/Microwave Test Engineer for a subassembly of the landing radar of the Mars Science Laboratory (due to be launched in 2011) in addition to co-designing the frequency synthesizer assembly of the Soil Moisture Active and Passive (SMAP) satellite radar.